

---

*Araştırma Makalesi / Research Article*

---

## **The Gray-level Co-occurrence Matrix Approach to Measure Uniformity of Fuji Prescale Pressure Sensitive Film Samples**

İbrahim MUTLU\*, Talip ÇELİK, Arif ÖZKAN, Yasin KİŞİOĞLU

*Kocaeli University, Department of Biomedical Engineering, Kocaeli  
(ORCID: 0000-0003-3864-3725) (ORCID:0000-0003-0033-2454)  
(ORCID:0000-0002-1288-6166) (ORCID:0000-0002-9819-2551)*

---

### **Abstract**

Fuji scaled pressure sensitive films (FPPSF) are used in many sciences, especially for mechanical-based measurements. Since these films are paper-based sensors, the measurement values are mostly found manually after a series of processing according to the ambient conditions. The accuracy of the measurement results depends on the calibration process. However, there is no determination method regarding the accuracy of these processes in the literature. The aim of this study is to point out the subjects that may affect the accuracy, especially during the experimental calibration and to recommend a new method in order to evaluate the homogeneity in particular. To evaluate the homogeneity of the calibration data produced for this purpose, the gray level co-occurrence matrix (GLCM) was used and statistically compared with the relevant calibration curves presented in the current literature. As a result, the energy property parameter of GLCM was found to be applicable to control the image smoothness of the samples to realize the accuracy of the generated curve.

**Keywords:** Image Uniformity Measurement, Fujifilm Prescale Pressure Sensitive Film, Calibration

---

## **Fuji Prescale Basınca Duyarlı Film Numunelerinin Homojenliğini Ölçmek İçin Gri Düzey Eş Oluşum Matrisi**

### **Öz**

Fuji önölçekli basınca duyarlı filmler (FPPSF) özellikle mekanik tabanlı ölçümler için birçok bilimdalında kullanılmaktadır. Bu filmler kağıt tabanlı sensör olduğu için ölçüm değerleri daha çok ortam şartlarına göre manuel olarak bir dizi işlemde sonra bulunur. Ölçüm sonuçlarının doğruluğu kalibrasyon sürecine bağlıdır. Ancak literatürde bu işlemlerin doğruluğu ile ilgili herhangi bir tayin yöntemi yoktur. Bu çalışmanın amacı özellikle deneysel olarak yapılan kalibrasyon esnasında doğruluğu etkileyebilecek noktaları işaret edip özellikle homojenliği değerlendirmek için yeni bir yöntem tavsiye verilmesidir. Bu amaçla üretilen kalibrasyon verilerinde homojenliğini değerlendirmek için gri düzey eş-oluşum matrisi (GLCM) kullanılarak mevcut literatürde sunulan ilgili kalibrasyon eğrileriyle istatistiksel olarak karşılaştırılmıştır. Sonuç olarak, GLCM'nin enerji özellik parametresi, üretilen eğrinin doğruluğunu gerçekleştirmek için örneklerin görüntü düzgünlüğünü kontrol etmek için uygulanabilir olduğu bulunmuştur.

**Anahtar kelimeler:** Resim Homojenlik Ölçümü, Fujifilm Önölçekli Basınca Duyarlı Film, Kalibrasyon.

---

### **1. Introduction**

Fuji prescale pressure sensitive films (FPPSF) (Fuji Photo Film Co., Ltd., Japan) have been used to measure both the contact areas and the pressure distributions between contact surfaces in many applications such as fishing [1], automotive[2-4], industry [5, 6] and particularly biomechanics [7-17]. FPPSF consists of two paper-based sheets of which features are described in detail by Liggins et al. [24] and Muturi et al. [25]. FPPSF carries out the measurement of the contact pressure distributions and the

---

\*Corresponding author: [ibrahim.mutlu@kocaeli.edu.tr](mailto:ibrahim.mutlu@kocaeli.edu.tr)

Received: 02.08.2019, Accepted: 01.07.2021

contact areas via the intensity of red stains. FPPSF provides optical stains that can be observably converted to applied pressure itself according to the optical comparison charts supplied by the manufacturer. Contact pressure distributions between the surfaces can also be calculated using FPPSF recordings with the techniques of digital image-processing. Pressure distribution quantity is determined regarding image intensities related to contact pressures by means of a calibration procedure. The calibration stains of this calibration procedure emerge by applying loads to film samples compressed between contact flat surfaces at areas the value of which is known [24, 25]. FPPSFs can be used to determine the contact pressure distributions of many biological joints such as knee [7, 8], hip [9, 11, 16], ankle [12, 17] and wrist [10] etc. apart from their other functions. FPPSFs have some advantages for biomechanical applications, in particular, pressures between irregular contact surfaces [26]. The shapes and dimensions of FPPSFs can be designed easily by cutting in an appropriate way with the geometry of the contact areas.

Many researchers generally calibrate their FPPSFs considering calibration method developed by Liggins et al. [24] in order to compute the concentration of the red stains [11-14, 16, 24, 25, 27-29]. The calibration data are produced by applying different loads using universal testing machine and are plotted as a function of optical density. Researchers usually conduct a regression analysis to get a specific calibration curve. Many researchers report a correlation coefficient of regression analysis in their studies [1, 12, 25, 26, 29]. Measured data in mid-values of the calibration data are estimated according to the calibration curve using interpolation technique. Many factors such as sample preparation, sample collection, random errors, etc. affect the accuracy of the measured data and cause the uncertainty of the developed model. One of these factors is the uniform distribution of stains in the calibration samples. Even though sample uniformity is not discussed in the literature for FPPSF, image uniformity of calibration samples also affect the accuracy of data. In a common sense, the generated model should be defined at a 95% confidence level. Therefore, a calibration of FPPSF must be validated to confirm the measured results. The validation process should be implemented to check the accuracy with a valid curve defined depending on environmental conditions. Nevertheless, in the available literature, researchers do not validate their calibration curves gained using the FPPSFs.

In this study, a calibration curve of FPPSF is generated by performing a set of calibration tests and applying pressures between 2.5-10 MPa using a cylindrical hardened-steel punch and a smooth surface. The confirmation of the calibration curve obtained experimentally is done, since eliminating errors for the curve accuracy is of paramount importance in a subsequent study. Therefore, as a new method, the gray-level co-occurrence matrix was used to evaluate the uniformity of the sample stains for quantitative evaluation of uniform distribution of the sample stains. Also, the generated curve is compared statistically with the related literature and validated empirically.

## 2. Materials and Methods

### 2.1. Experimental Calibration of the FPPSF

The calibration tests using FPPSF samples are performed in this study by a polished hardened steel punch with a diameter of 30 mm and a metal plate surface to obtain uniform pressure distribution. The contact surfaces of the steel punch and metal base plate are grinded well before polishing on account of the fact that FPPSF is very sensitive to surface roughness. The apparatus of the calibration tests are shown in Fig. 1. As seen from the figure, a spherical guide in a small spherical cavity on the punch is used to avoid eccentric loading effects during the tests. These steps are taken into account to obtain uniformly distributed stains on the calibration samples. The tests are performed using a hydraulic press having a ton capacity of a load cell and the loads of 180, 270, 360, 450, 540, 630, and 720 kgf (1 kgf = 9.80 N) are applied to the samples, then made to wait and released for a 5-second per each. The stained images on the film are scanned by a scanner, (Mustek 1248UB), with a 600x600 dpi resolution as seen in Fig. 2. The tests are performed under environmental conditions of 42%±3 Rh humidity and 19±1°C temperature. Based on the calibration tests, a low-grade FPPSF with the capacity of 2.5-10 MPa is used in our biomechanical study to measure the contact areas and pressure distributions.

Undesired artefacts at the outer area of the scanned images are wiped out using an eraser tool called as “Erase Method” defined by Bachus et al. in view of the fact that the artefacts affect average values of the grayscale level as shown in Fig. 3 [30]. As seen in the figure, the pressure images are

converted to grayscale form by MATLAB software and then filtered with a 25x25 pixels averaging filter to remove noises. The noise in the pressure images is assumed to cause variations of the pixel values that are not related with the outer area pixels. The average values of the grayscale optical density are considered regardless of neighbouring pixels and plotted with respect to the applied pressure as illustrated in Fig. 4.

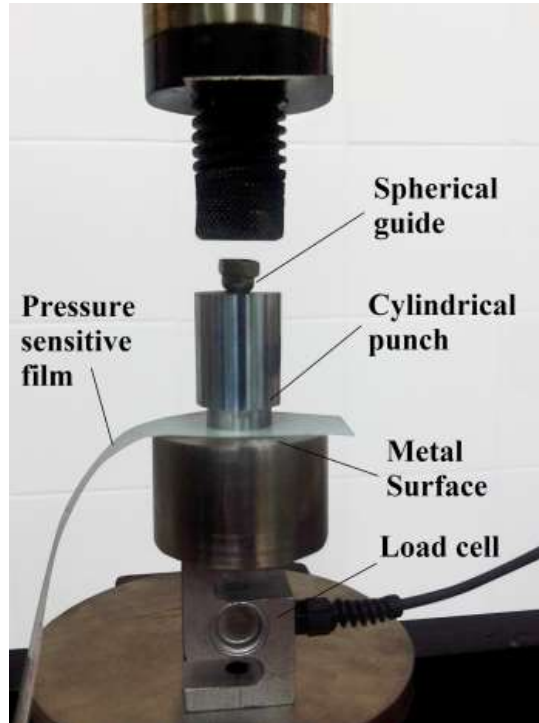


Figure 1. The compression test with a hydraulic universal press



Figure 2. The red stains images of the samples subjected to different loads

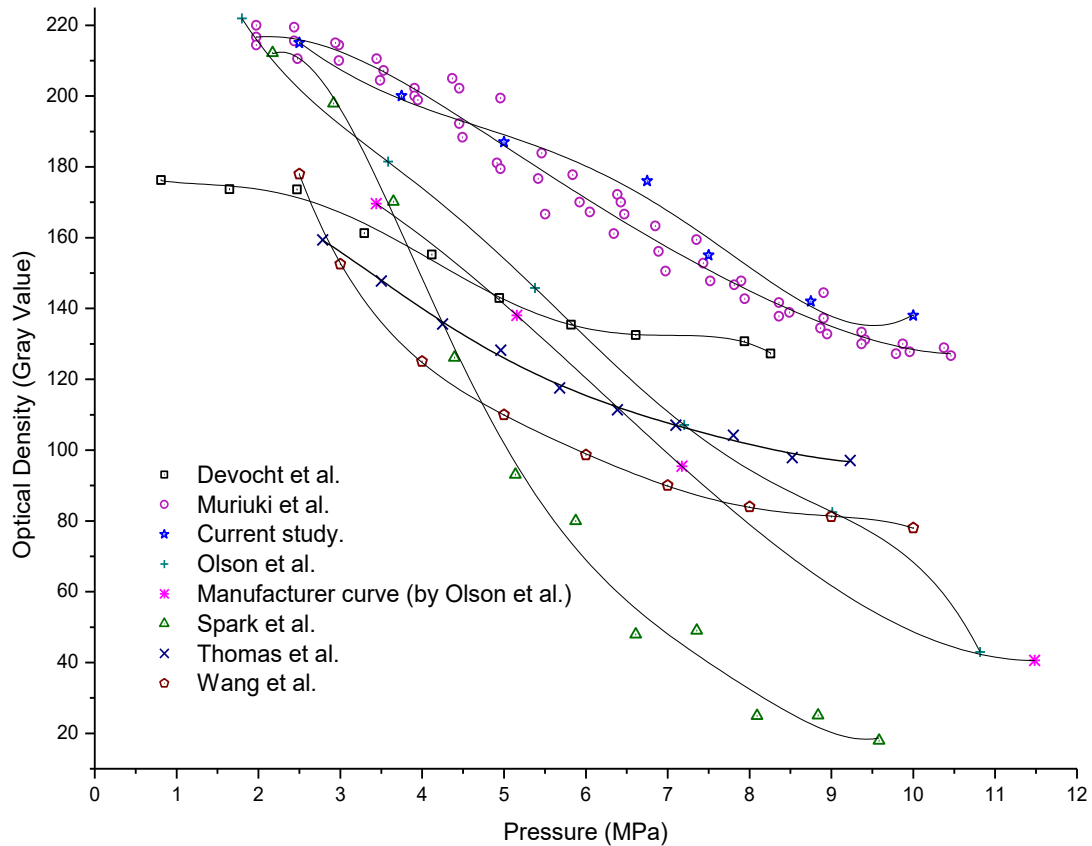


Figure 3. Obtaining the grayscale of the images using “Erase method”

## 2.2. Comparisons of the Calibration Curves

The calibration data for low and super-low grade FPPSF developed by researchers are extracted and plotted as a function of applied pressures as illustrated in Fig. 4 and 5, respectively [11, 14, 16, 24, 25, 27, 28]. The scanned images are converted to 8 bpp (8 bit-per-pixel) grayscale pixel values to represent the level of grayness and brightness ranging from black to white, sometimes called as monochrome. The converted digital images in the grayscale are generally defined black and white levels as respectively zero and 255 (maximum value), by researchers. In contrast, Olson et al. [16] and Devocht et al. [14]

defined black and white points as 255 and zero, respectively. Both of the data are extracted and converted into the same grayscale format in this study. Their calibration curves are generated after collecting all data using a fifth-order polynomial equation to get the best fit to the characteristic of the curves [24] given in Fig. 4 and 5. As seen, notwithstanding the same FPPSF, the calibration curves have different characteristics. Thus, calibration tests and image process techniques must be questioned for the differences among the curves.



**Figure 4.** The generated and published calibration data for low-grade FPPSF

One of these reasons depends on environmental conditions. In Fig. 4 and 5, the calibration curves appear to be highly dependent on environmental conditions such as load-rate, ambient temperature and relative humidity which affect red stain intensity during the tests. In addition, the manufacturer of the FPPSFs provides different calibration charts based on environmental conditions [31]. Therefore it is assumed that the calibration curve obtained in this experiment is also derived and plotted as function of pressure and optical density depending on low and high ambient temperatures and humidity as given in Fig. 6 considering the manufacturer's chart. As seen in the figure, the obtained optical density values are matched with the stain density values given in the chart. These curves are plotted as a function of pressure and optical density in order to understand the temperature and humidity effects on FPPSF easily. The optical density values of the curves for low pressures are close to each other than those for high pressures. The calibration curves show different behaviours as researchers may be performed their tests under different environmental conditions. Processing parameters of the calibration tests carried out by the researchers are summarized in Table 1.

Our calibration curve is closely matched with the curve developed for 56 test data by Muriuki et al. [25] as given in Fig. 4. When compared, the calibration curve of Muriuki et al. might be regarded as a suitable curve due to plenty of data even if the environmental conditions are not stated. The accuracy of this curve is more sensitive than the others [25]. Although test conditions are unknown as listed in Table 1., calibration curves developed by Wang et al. [28], Thomas et al. [12], and Devocht et al. [14] have a similar (Fig. 6) proportionality to each other but not overlapped. This indicates that they studied under different experimental environmental conditions. Olson et al. [16] stated that their calibration curve agrees well with low-humidity conditions based upon reference data supplied by the manufacturer.

A similar proportionality can also be seen among the curves published by Spark et al. [10], Olson et al. [16], and Muriuki et al. [25] as given in Fig. 4. In addition, the curves developed in different environmental conditions by Liggins et al.[24, 27] demonstrate similar behaviour in Fig. 5.

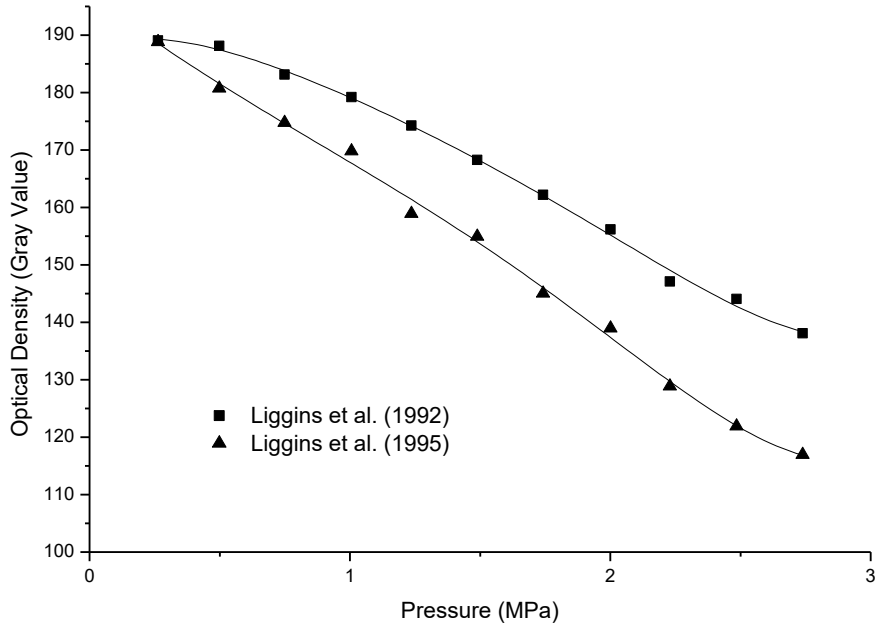


**Figure 5.** The published calibration data for super-low grade FPPSF

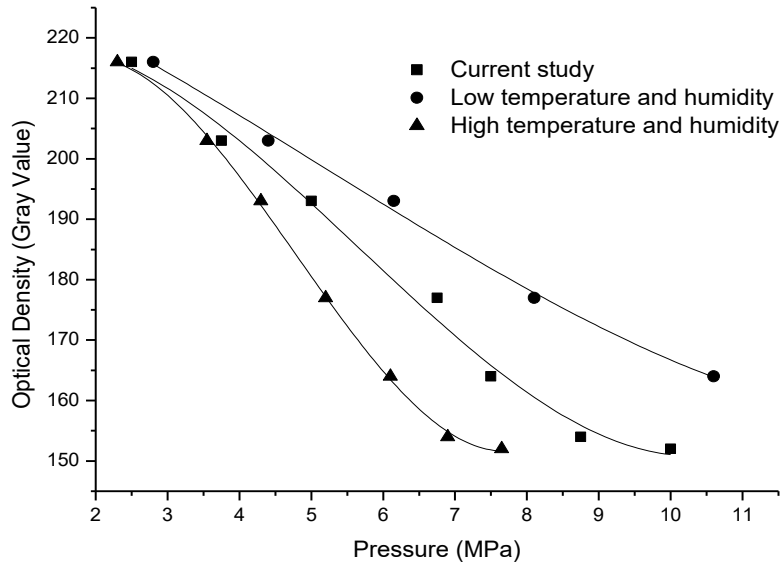


**Figure 6.** The calibration curves for different environmental conditions

### 2.3. Statistical analysis

The statistical relationships between the obtained and published curves are computed by a coefficient of regression [32],  $R^2$ , reflecting the percentage of variability among the curves given in Fig. 4 and 5. These curves are analysed by deriving curve equation and compared statistically using SPSS software (R16). Based on the comparisons, the  $r^2$  coefficient of our curve is complied with 95% prediction intervals of the curve published by Muriuki et al. [25]. The rest of the curves (see Fig. 4 and 5) shows significant differences ( $p < 0.001$ ) from each other.

**Table 1.** Processing parameters of the experimental conditions and image acquisitions

References	Temp. °C	Humidity %	Loading Rates	Scanner Device	Resolution	Software
Liggins et al. [24]	25±3	42.5 ±3	60	CCD video camera		Image Pro II
Liggins et al. [27]	23±1	48	60	CCD video camera		Image Pro +
Muriuki et al. [25]				HpScanjet 5550 c	600 dpi	MATLAB
Current study	19±1	42% ±3	5	MUSTEK 1248UB	600 dpi	MATLAB
Spark et. al. [11]			60	HpScanjet 11cx/T		Bioquant
Olson et al. [16]	Lab. condition	35		Abaton Scan	2,95 pixel/mm	
Thomas et al. [12]			5	Densitometer FPD-305	300 dpi	
Wang et al. [28]			5		65x5 pixel/cm	
Devocht et al. [14]				Digital Camera		NIH Image 1,55

In order to provide relatively uniform stains on the FPPSF, various precautions is provided in the experimental study, such as by polishing and grinding punch and metal base to avoid poor dusting of them and by using a spherical guide in a small spherical cavity on the punch to avoid eccentric loading. Nevertheless non-uniform distribution or fluctuation in the intensity had been occurred in some sample cases and rejected for inclusion to calibration curve. The density distribution of the calculated samples was visually assessed and find acceptable relatively for the calibration curve. For quantitative evaluation of uniform distribution of the sample stains, the gray-level co-occurrence matrix was used to evaluate the uniformity of the sample stains. This matrix is a statistical method to analyse the texture of the image and sometimes called Haralick features [33]. The uniformity was measured in all samples with the energy property of this matrix using MATLAB software. The calculated values are given in Table 2. The value changes from 0 to 1 and the energy value for 1 means constant image. Also, to examine the deviation by comparing the uniformity value and the random error of data in the regression analysis, the random errors ( $\epsilon$ ) of data was added to Table 2. Energy indicator is a measure of uniformity of an image. A high value indicates a uniform distribution. The ideal homogeneity is represented by 1. Thus, data on the homogeneity of sample stains is obtained. Whether the sample can be used to generate the calibration curve is acquired.

**Table 2.** The values for image uniformity for all samples

Load (kgf)	180	270	360	450	540	630	720
Energy	0.7671	0.3886	0.5052	0.3331	0.6492	0.4016	0.5215
Random error of optical density ( $\epsilon$ )	-0.1693	0.9432	-2.16	4.4517	-5.5135	-0.0246	-0.14

When the energy indicators in Table 2 are examined, it is understood that the homogeneity of samples 2 and 4, which is less than 0.5, is low. When the samples are examined visually, the accuracy of the numerical expressions is appeared.

### 3. Discussion

Adequate overall comparisons among the calibration curves in published article have not been made to fill the gap in literature yet. Chin et al. compared their data with the conventional calibration images provided by the manufacturer without the report of accuracy measurement [15]. Olson et al. compared their calibration curve with a curve supplied by the manufacturer [16]. The limitations in FPPSF in terms of performance and accuracy were compared with K-Scan and I-Scan systems by Harris et al. [34] and Bachus et al. [30], respectively.

Bachus et al. [30] used a calibration technique described by Liggins et al. [24] to validate their calibration data using I-scan system. Hasler et al. [26] compared their calibration curves obtained for flat and curved surfaces in stable environmental conditions. They used a non-linear least-square algorithm to fit the curves and a non-linear multiple regression model to compare statistically. Muriuki et al. [25] studied to validate the image processes of FPPSF using his own software and gained an accuracy level lower than 10%. However, no comprehensive analysis in terms of comparisons has been conducted in literature to emphasize the accuracy of calibration curves except the study of Olson et al. whose comparison is inadequate [16]. In our study, a comprehensive comparison is performed between our curve and corresponding curves published in literature. This graphical comparison may help to understand to get a desired accuracy of the calibration procedure of FPPSF to be used in a subsequent study. Therefore, the comparison and statistical analyses of the curves indicate how the environmental conditions affect the calibration curves (see Fig. 6).

Many various factors affecting the calibration curve ought to be classified in two groups. One of them can be defined as image processes such as scanning resolutions, scanner linearity, filtering effects, etc. [35, 36]. These factors absolutely affect the grayscale quality indistinguishably. The other one is related with the environmental conditions of experimental applications such as humidity, temperature and loading time [31]. In addition, polynomial regression degree of the calibration curve can affect the results [37]. The reasons of the differences among the curves (in Fig. 4 and 5) can be interpreted easily with regard to the FPPSF manual when the environmental conditions of the tests are explained in the publications. Hence, the processing parameters of the test conditions should be stated in the publications for better assessment. The curves in Fig. 6 are different from each other due to the factors mentioned above, in spite of a marginal similarity and conformity among them. For these reasons, the calibration curve for FPPSF should be validated empirically.

Liggins et al. reported a method for an analysis of stain resolution [38]. In similar study, Liggins et al. aimed to quantify the effects of an image-enhancement on the resolution properties of pressure maps [39]. Also the standard deviation of pixel-values was presented and random granularity was mentioned for the first time. This factor affects the uniformity of FPPSF. But it was not quantified. Singerman et al. introduced an experimental technique of FPPFS for use in small areas [40]. Singerman conducted the intensity frequency distribution of pixel gray levels as a statistic method. Though calculated parameters and given graphs cause us to think sample uniformity, a clear hint was not presented about the sample uniformity. In present study, we focused also sample uniformity and this factor previously was not directly stated in any paper. Non-uniform distribution is obviously seen in the second and fourth samples in visual inspection of samples in Fig 2. With a glance at image uniformity values in Table 2, the values of image uniformity results seem compatible with visual inspection. Due to this, the parameter of energy property of gray-level co-occurrence matrix can be practicable to check the image uniformity of samples. Also, the most discreteness can be seen in fourth sample that disarrayed the linearity of the calibration curve in the Fig. 4. Random error of optical density data ( $\epsilon$ ) can give tips for excessive discreteness. When taking a look at table 2., fourth and fifth samples was found to be highest error on the residuals. If fourth sample would be uniform, fifth sample probably could fit with calibration curve. Hence we can supposedly say that the parameter of energy property of gray-level co-occurrence matrix can be useful for determining the uniformity of samples. This parameter can make

contribution to desired accuracy of FPPSF on processing of fitting calibration curve.

#### **4. Conclusion**

The current study addresses the congruity or ratio among curves reported in literature. The results of the experimental studies are computed based on the calibrated curves of FPPSF that is fundamental for a subsequent study. Nonetheless, the published curves have no foundation in order to confirm the accuracy. The indication of this is the nonconvergency of the curves to each other. But the curves must be convergent at a minimum pressure level, at least, according to the FPPSF manual. Taking these into account, we can conclude that the ambient temperature and relative humidity play a critical role in changing the calibration curves. For these reasons, the evaluation of the contact pressure distribution and the contact area in the studies has certain deviations from a desired accuracy. In the next step, the GLMC homogeneity study should be requested from the investigators to ensure the accuracy of the results during the FPPS calibration run. Thus, reference data on the general calibration method or the uniformity of the samples can be recommended. A set of guidelines or standards for the calibration process must be set to create a precise calibration curve based on the commonalities and correlations among literature publications.

#### **Acknowledgements**

This work was supported by the Scientific Research Projects Unit of Kocaeli University under project no. 2015/098

#### **Author's Contributions**

I. Mutlu. and T. Celik performed experiments and prepared the manuscript, A. Ozkan and Y. Kisioglu analysed and discussed the manuscript.

#### **Statement of Conflicts of Interest**

There is no conflict of interest among the authors.

#### **Statement of Research and Publication Ethics**

The authors declare that this study complies with Research and Publication Ethics.

#### **References**

- [1] Cada G., Smith J., Busey J. 2005. Use of Pressure-Sensitive Film to Quantify Sources of Injury to Fish. *North American Journal of Fisheries Management*, 25:57-66.
- [2] Bakar A., Ouyang H., Siegel J.E. 2005. Brake pad surface topography Part I: contact pressure distribution. *SAE Technical Paper*, 2005-01-3941.
- [3] Costanzi M., Rouillard V., Cebon D. 2006. Effects of tyre contact pressure distribution on the deformation rates of pavements. *Proceedings of the 19th Symposium of the International Association for Vehicle System Dynamics: Taylor and Francis*,. p. 892-903.
- [4] Joo, B. S., Gweon, J., Park, J., Song, W., Jang, H. 2021. The effect of the mechanical property and size of the surface contacts of the brake lining on friction instability. *Tribology International*, 153, 106583.
- [5] Aymerich F, Pau M, Ginesu F. 2003. Evaluation of Nominal Contact Area and Contact Pressure Distribution in a Steel-Steel Interface by Means of Ultrasonic Techniques. *JSME International Journal Series C Mechanical Systems, Machine Elements and Manufacturing*, 46:297-305.
- [6] Lee C-Y., Lin C-S., Jian R-Q., Wen C-Y. 2006. Simulation and experimentation on the contact width and pressure distribution of lip seals. *Tribology International*, 39:915-20.

- [7] Cheng C.K, Huang C.H, Liao J.J. 2003. The influence of surgical malalignment on the contact pressures of fixed and mobile bearing knee prostheses--a biomechanical study. *Clinical Biomechanics*, 18:231-6.
- [8] Wolchok J.C., Hull M.L., Howell S.M. 1998. The effect of intersegmental knee moments on patellofemoral contact mechanics in cycling. *Journal of Biomechanics*, 31:677-83.
- [9] Konrath G.A., Hamel A.J., Olson S.A., Bay B., Sharkey N.A. 1998. The role of the acetabular labrum and the transverse acetabular ligament in load transmission in the hip. *The Journal of bone and joint surgery American volume*, 80:1781-8.
- [10] Skie M., Grothaus M., Ciocanel D., Goel V. 2007. Scaphoid excision with four-corner fusion: a biomechanical study. *Hand*, 19:4-8.
- [11] Sparks D.R., Beason D.P., Etheridge B.S., Alonso J.E., Eberhardt A.W. 2005. Contact pressures in the flexed hip joint during lateral trochanteric loading. *Journal of orthopaedic research*, 23:359-66.
- [12] Thomas J.L., Moeini R., Soileau R. 2000. The effects on subtalar contact and pressure following talonavicular and midtarsal joint arthrodesis. *The Journal of Foot and Ankle Surgery*, 39:78-88.
- [13] Field J.R., Hearn T.C., Caldwell C.B. 1998. The influence of screw torque, object radius of curvature, mode of bone plate application and bone plate design on bone-plate interface mechanics. *Injury*. 29:233-41.
- [14] Devocht J.W., Goel V.K., Zeitler D.L., Lew D. 2001. Experimental validation of a finite element model of the temporomandibular joint. *Journal of oral and maxillofacial surgery*, 59:775-8.
- [15] Chin M.V., Donohue J.M., Erdman A.G., Oegema T.R., Thompson R.C. 1986. Biomechanical Analysis of an Adult Canine Patella under an indirect Blunt Trauma. *ORS Trans*, 11.
- [16] Olson S.A., Bay B.K., Chapman M.W., Sharkey NA. 1995. Biomechanical consequences of fracture and repair of the posterior wall of the acetabulum. *The Journal of bone and joint surgery American volume*, 77:1184-92.
- [17] Wang C-L., Cheng C-K., Chen C-W., Lu C-M., Hang Y-S., Liu T-K. 1995. Contact areas and pressure distributions in the subtalar joint. *Journal of Biomechanics*, 28:269-79.
- [18] Horibe, Y., Matsuo, K., Ikebe, K., Minakuchi, S., Sato, Y., Sakurai, K., Ueda, T. 2021. Relationship between two pressure-sensitive films for testing reduced occlusal force in diagnostic criteria for oral hypofunction. *Gerodontology*.
- [19] Bobko, A., Edwards, G., Rodriguez, J., Southworth, T., Miller, A., Peresada, D., Goldberg, B. 2021. Effects of implant rotational malposition on contact surface area after implantation of the augmented glenoid baseplate in the setting of glenoid bone loss. *International Orthopaedics*, 1-6.
- [20] Gu, Y., Bai, Y., Xie, X. 2021. Bite Force Transducers and Measurement Devices. *Frontiers in Bioengineering and Biotechnology*, 9, 253.
- [21] Saiz, A., Delman, C. M., Haffner, M., Wann, K., McNary, S., Szabo, R. M., Bayne, C. O. 2021. The Biomechanical Effects of Simulated Radioscapholunate Fusion with Distal Scaphoidectomy, 4-Corner Fusion with Complete Scaphoidectomy, and Proximal Row Carpectomy Compared to the Native Wrist. *The Journal of Hand Surgery*.
- [22] Idris, R. I., Shoji, Y., Lim, T. W. 2021. Occlusal force and occlusal contact reestablishment with resin-bonded fixed partial dental prostheses using the Dahl concept: A clinical study. *The Journal of prosthetic dentistry*.
- [23] Ayna, M., Karayürek, F., Jepsen, S. Emmert M., Acil Y., Wiltfang J., Gülses A., 2021. Six-year clinical outcomes of implant-supported acrylic vs. ceramic superstructures according to the All-on-4 treatment concept for the rehabilitation of the edentulous maxilla. *Odontology*, 109(4), 930–940.
- [24] Liggins A.B., Stranart J.C.E., Finlay J.B., Rorabeck C.H. 1992. Calibration and Manipulation of Data from Fuji Pressure-Sensitive Film. *Clin Asp B.*, 3:61-70.
- [25] Muriuki M.G., Gilbertson L.G., Harner C.D. 2009. Characterization of the performance of a custom program for image processing of pressure sensitive film. *Journal of biomechanical engineering*, 131(1):014503.
- [26] Hasler E.M., Herzog W., Fick G.H. 1996. Appropriateness of plane pressure-sensitive film calibration for contact stress measurements in articular joints. *Clinical Biomechanics*, 11(6):358-360.

- [27] Liggins A.B., Surry K, Finlay J.B. 1995. Sealing Fuji Prescale pressure sensitive film for protection against fluid damage: the effect on its response. *Strain*, 31:57-62.
- [28] Wang C.L., Cheng C.K., Chen C.W., Lu C.M., Hang Y.S., Liu T.K. 1995. Contact areas and pressure distributions in the subtalar joint. *Journal of Biomechanics*, 28(3):269-279.
- [29] Mutlu I., Ugur L., Celik T., Buluc L., Muezzinoglu U.S., Kisioglu Y. 2014. Evaluation of contact characteristics of a patient-specific artificial dysplastic hip joint. *Acta Bioeng Biomech*, 16:111-120.
- [30] Bachus K.N., DeMarco A.L., Judd K.T., Horwitz D.S., Brodke D.S. 2006. Measuring contact area, force, and pressure for bioengineering applications: using Fuji Film and TekScan systems. *Medical Engineering & Physics*, 28:483-488.
- [31] Fuji Photo Film Co. Ltd. Pressure measuring film-FUJI prescale film instruction manual.
- [32] Introduction to SAS. UCLA: Statistical Consulting Group; 2013.
- [33] Haralick R.M, Shanmugam K., Dinstein I. 1973. Textural features for image classification. *IEEE Transactions on Systems, Man and Cybernetics*, Smc3:610-621.
- [34] Harris M.L., Morberg P., Bruce W.J.M., Walsh W.R. 1999. An improved method for measuring tibiofemoral contact areas in total knee arthroplasty: a comparison of K-scan sensor and Fuji film. *Journal of Biomechanics*, 32:951-958.
- [35] Balter S. 1993. Fundamental properties of digital images. *Radiographics*, 13:129-141.
- [36] Spring K.R., Russ J.C., Davidson M.W. Basic Properties of Digital Images, Concepts in Digital Imaging Technology. Hamamatsu Learning Center.
- [37] Mutlu I., Kisioglu Y. 2013. Higher order regression functions result better fit for the calibration curve. *Journal of Orthopaedic Research*, 31:1164-.
- [38] Liggins A.B., Hardie W.R., Finlay J.B. 1995. The spatial and pressure resolution of Fuji pressure-sensitive Film. *Experimental Mechanics*., 35:166-173.
- [39] Liggins A.B., Finlay J.B. 1997. Image-averaging in the analysis of data from pressure-sensitive film. *Exp Techniques*, 21:19-22.
- [40] Singerman R., Pedersen D., Brown T. 1987. Quantitation of pressure-sensitive film using digital image scanning. *Experimental Mechanics*, 27:99-105.